HHS Public Access

Author manuscript

Brain Behav Immun. Author manuscript; available in PMC 2019 October 01.

Published in final edited form as:

Brain Behav Immun. 2018 October ; 73: 364–374. doi:10.1016/j.bbi.2018.05.021.

TRIF is a key inflammatory mediator of acute sickness behavior and cancer cachexia

Kevin G. Burfeind[1,2], **Xinxia Zhu**[1], **Peter R. Levasseur**[1], **Katherine A. Michaelis**[1,2], **Mason A. Norgard**[1], and **Daniel L. Marks**[1,3,*]

[1]Papé Family Pediatric Research Institute, Oregon Health & Science University, Portland, OR USA

[2]Medical Scientist Training Program, Oregon Health & Science University, Portland, OR USA

[3]Knight Cancer Institute, Oregon Health & Science University, Portland, OR USA

Abstract

Hypothalamic inflammation is a key component of acute sickness behavior and cachexia, yet mechanisms of inflammatory signaling in the central nervous system remain unclear. Previous work from our lab and others showed that while MyD88 is an important inflammatory signaling pathway for sickness behavior, MyD88 knockout (MyD88KO) mice still experience sickness behavior after inflammatory stimuli challenge. We found that after systemic lipopolysaccharide (LPS) challenge, MyD88KO mice showed elevated expression of several cytokine and chemokine genes in the hypothalamus. We therefore assessed the role of an additional inflammatory signaling pathway, TRIF, in acute inflammation (LPS challenge) and in a chronic inflammatory state (cancer cachexia). TRIFKO mice resisted anorexia and weight loss after peripheral (intraperitoneal, IP) or central (intracerebroventricular, ICV) LPS challenge and in a model of pancreatic cancer cachexia. Compared to WT mice, TRIFKO mice showed attenuated upregulation of *Il6*, *Ccl2*, *Ccl5*, *Cxcl1*, *Cxcl2*, and *Cxcl10* in the hypothalamus after IP LPS treatment, as well as attenuated microglial activation and neutrophil infiltration into the brain after ICV LPS treatment. Lastly, we found that TRIF was required for *Ccl2* upregulation in the hypothalamus and induction of the catabolic genes, *Mafbx*, *Murf1*, and *Foxo1* in gastrocnemius during pancreatic cancer. In summary, our results show that TRIF is an important inflammatory signaling mediator of sickness behavior and cachexia and presents a novel therapeutic target for these conditions.

Keywords

Cachexia; neuroinflammation; hypothalamus; sickness behavior; neuroimmunology; microglia

[*]*Corresponding Author Information*, Daniel L. Marks, 3181 SW Sam Jackson Park Road, L 481, Portland, OR 97239, marksd@ohsu.edu.

Competing Interests

The authors have no competing interests to report.

1. Introduction

Innate immune activation in response to various pathogens leads to systemic and central nervous system (CNS) inflammation, inducing a distinct metabolic and behavioral paradigm that includes fever, weight loss, anorexia, and fatigue. This constellation of signs and symptoms, referred to as “sickness behavior” (Dantzer et al. 1998), is critical for combating infection and allows resources to be diverted to the immune system to fight pathogens. However, if sickness behavior is maintained in conditions of chronic inflammation, it can become maladaptive and manifest as cachexia. Cachexia is a devastating syndrome characterized by anorexia, increased catabolism of lean body mass, and lethargy (Argiles et al. 2010; Evans et al. 2008; Fearon et al. 2011). It is prevalent in numerous chronic diseases, including cancer (Tisdale 2002), chronic renal failure (Wang et al. 2004), congestive heart failure (Anker et al. 1997), and untreated HIV (Kotler et al. 1989). Furthermore, cachexia is associated with increased mortality of the underlying disease and decreased quality of life (Bachmann et al. 2008; Wesseltoft-Rao et al. 2015; Lainscak, Podbregar, and Anker 2007). Despite this serious clinical concern, there are currently no effective treatments and mechanisms remain controversial.

Our lab, along with others, described a CNS-based mechanism of cachexia in which cytokines generated in the periphery are amplified and modified within the hypothalamus, leading to aberrant activity of weight- and activity-modulating neurons (Braun et al. 2011; Burfeind, Michaelis, and Marks 2015; Bluthé et al. 2000). Specifically, intracerebroventricular (ICV) injection of inflammatory cytokines (Sonti, Ilyin, and Plata-Salaman 1996; Bodnar et al. 1989) or pathogen associated molecular patterns such as lipopolysaccharide (LPS) (Wisse et al. 2007) potently reduces food intake and activity. Furthermore, peripheral or central cytokine injection or immune challenge leads to rapid activation of neurons in areas that are critical for food intake and energy metabolism, such as the nuclei of the mediobasal hypothalamus (MBH) (Elmquist et al. 1996; Konsman, Tridon, and Dantzer 2000; Laflamme and Rivest 1999; Morgan and Curran 1986). However, the cellular and molecular pathways whereby peripheral inflammation is translated in the brain into behavioral or metabolic responses are still not well understood.

Toll-like receptors (TLRs) are key components of the innate immune system, recognizing a variety of pathogens and inflammatory signals. TLR function is important for mounting an appropriate inflammatory response, and metabolic signaling in the CNS is closely tied to TLR signaling (Jin et al. 2016). Pro-inflammatory signaling via the Myeloid Differentiation Primary Response Gene 88 (MyD88) pathway was initially thought to be the dominant mechanism whereby the binding of pathogenic signaling molecules to receptors is linked to the synthesis and release of inflammatory cytokines and chemokines (Medzhitov et al. 1998). However, recent data suggest that MyD88-independent pathways linking TLRs to cellular activation are present within the brain (Hanke and Kielian 2011; Lin et al. 2012). In our previous work, we found that while sickness behavior was severely attenuated in MyD88KO mice, a slight anorexia response was present and muscle catabolism occurred (Braun et al. 2013). The adaptor protein TIR-domain-containing adaptor inducing interferon-β (TRIF) is an important inflammatory signaling mediator, yet has received little attention in the context of CNS-mediated alterations in behavior and metabolism during

illness. TRIF is the dominant adapter for TLR3 signaling, and plays an essential role in TLR4 responses to LPS as well (Yamamoto et al. 2003). Furthermore, TRIF knockout (TRIFKO) mice are nearly as resistant to endotoxin-induced mortality as are MyD88KO mice (Feng et al. 2011).

The role of TRIF signaling in the CNS during acute sickness behavior and cachexia is unknown. We found that TRIF signaling is important for neuroinflammation and resulting acute sickness behavior after systemic or central exposure to LPS. We also found that mice lacking TRIF have attenuated cancer cachexia. These results implicate TRIF as a key signaling mediator in inflammation-driven behavioral and metabolic changes during illness, and a potential therapeutic target for cachexia.

2. Materials and Methods

2.1 Animals

Male and female 20–25-g WT C57BL/6J (stock no. 000664), MyD88KO (stock no. 009088), TRIFKO ($Trif^{Lps2}$, stock no. 005037) mice were obtained from The Jackson Laboratory. No immune, developmental, or behavioral abnormalities were observed in TRIFKO mice by our group, consistent with the existing literature (Yamamoto et al. 2003; Zhu et al. 2016). Furthermore, they consume the same amount of food as WT animals in the absence of inflammation (see Figs 2 and 3), and their spleens are the same size (data not shown). Mice were between 7 and 12 weeks of age at time of experiment. All animals were maintained at 27°C on a normal 12:12 hr light/dark cycle and provided *ad libitum* access to water and food. Experiments were conducted in accordance with the National Institutes of Health Guide for the Care and Use of Laboratory Animals, and approved by the Animal Care and Use Committee of Oregon Health and Science University.

2.2 Intracerebroventricular Cannulation and Injections

Mice were anesthetized under isoflurane and placed on a stereotactic alignment instrument (Kopf Instruments, CA). 26-gauge lateral ventricle cannulas were placed at −1.0 mm X, −0.5 mm Y, and −2.25 mm Z relative to bregma. Injections were given in 2 μl total volume. LPS (from *Escherichia coli*, O555:B5, Sigma Aldrich, St. Louis, MO) was dissolved in normal saline with 0.5% bovine serum albumin.

2.3 Nocturnal Feeding Studies

Animals were transferred to clean cages and injected with ICV (50 ng) or IP (250 μg) LPS 1 h prior to lights off. At 2, 6, 12, 24, 36 and 48 hrs after the onset of the dark cycle, food was weighed and returned to the cage. Body weight was recorded at 12, 24, 36, and 48 hrs.

2.4 Plasma Corticosterone Measurement

Plasma corticosterone levels were measured by RIA (MP Biomedicals, Valiant, Yantai, China) according to the manufacturer’s instructions. Animals were anesthetized with a lethal dose of a ketamine/xylazine/acetapromide 4 hrs after IP LPS administration. Blood was obtained by cardiac puncture, anticoagulated with EDTA and separated by centrifugation. Plasma was stored at −80°C until analysis.

2.5 Quantitative Real-Time PCR

Prior to tissue extraction, mice were euthanized with a lethal dose of a ketamine/xylazine/acetapromide and sacrificed. Hypothalamic blocks were dissected, snap frozen, and stored in −80 °C until analysis. Hypothalamic RNA was extracted using an RNeasy mini kit (Qiagen, Hilden, Germany) according to the manufacturer's instructions. cDNA was transcribed using TaqMan reverse transcription reagents and random hexamers according to the manufacturer's instructions. PCR reactions were run on an ABI 7300 (Applied Biosystems, Foster City, CA), using TaqMan universal PCR master mix with the following TaqMan mouse gene expression assays, selected based on previous studies from our lab and others which showed their importance in sickness behaviors and cachexia (Braun et al. 2011; Zhu et al. 2016; Le Thuc et al. 2017): *18s* (Mm04277571_s1), *Il1b* (Mm00434228_m1), *Tnf* (Mm00443258_m1), *Il6* (Mm01210732_g1), *Cd80* (Mm00711660_m1), *Myd88* (Mm00440338_m1), *Ifnβ* (Mm00439552_s1), *Ccl2* (Mm99999056_m1), *Ccl5* (Mm01302427_m1), *Cxcl1* (Mm04207460_m1), *Cxcl2* (Mm00436450_m1), *Cxcl10* (Mm00445235_m1), *Gapdh* (Mm99999915_g1), *Mafbx* (Mm00499518_m1), *Murf1* (Mm01185221_m1), and *Foxo1* (Mm00490672_m1). It is important to note that *Ifnβ* is a single exon gene and therefore results may be confounded by genomic DNA. However, we used DNAse to eliminate genomic DNA and also ran a no-primer control, which showed no amplification (not shown).

Relative expression was calculated using the ΔΔCt method and normalized to WT vehicle treated or sham control. Statistical analysis was performed on the normally distributed ΔCt values.

2.6 Immunohistochemistry

Mice were anesthetized using a ketamine/xylazine/acetapromide cocktail and sacrificed by transcardial perfusion fixation with 15 mL ice cold 0.01 M PBS followed by 25 mL 4% paraformaldehyde (PFA) in 0.01 M PBS. Brains were post-fixed in 4% PFA overnight at 4°C and cryoprotected in 20% sucrose for 24 hrs at 4°C before being stored at −80°C until used for immunohistochemistry. Immunofluorescence histochemistry was performed as described below. Free-floating sections were cut at 30 μm from perfused brains using a sliding microtome (Leica SM2000R, Leica Microsystems, Wetzlar, Germany). Hypothalamic sections were collected from the division of the optic chiasm (bregma −1.0 mm) caudally through the mammillary bodies (bregma −3.0 mm). Sections were incubated for 30 min at room temperature in blocking reagent (5% normal donkey serum in 0.01 M PBS and 0.3% Triton X-100). After the initial blocking step, sections were incubated in rabbit anti-mouse Iba-1 (1:500, DAKO) in blocking reagent for 24 hrs at 4°C, followed by incubation in donkey anti-rabbit Alexa 555 (1:1000) for 2 hrs at room temperature. Between each stage, sections were washed thoroughly with 0.01 M PBS. Sections were mounted onto gelatin-coated slides and coverslipped using Prolong Gold Antifade media with DAPI (Thermofisher, Waltham, MA).

2.7 Microglia Activation Quantification

Microglia activation in the MBH was quantified using Fiji (ImageJ, NIH, Bethesda, MD). The MBH was defined as the region surrounding the third ventricle at the base of the brain,

starting rostrally at the end of the optic chiasm when the arcuate nucleus appears (−1.22 mm from bregma) and ending caudally at the mammillary body (−2.70 mm from bregma). Images were acquired using the 20× objective (na = 0.8, step size = 1 μm) with a 10× ocular zoom, resulting in 200× magnification. The base of the MBH was positioned at the very bottom of the field of view (FOV) and the third ventricle at the center of the FOV. Care was taken to exclude the meninges so as to avoid analysis of meningeal macrophages. Images were 2048×2048 pixels, with a pixel size of 0.315 μm. Images were acquired as 8-bit RGB TIFF images. 3–10 MBH images per animal were acquired and analyzed by a researcher blinded to genotype and treatment group (KGB).

After image acquisition, TIFF images were uploaded to Fiji and converted to 8-bit greyscale images. After thresholding, microglia were identified using the Analyze Particle function, which measured mean Iba-1 fluorescent intensity per cell and cell area. Iba-1 fluorescent intensity and cell size was measured for each microglia in the arcuate nucleus. Due to the density of microglia in the median eminence (ME), the software was unable to differentiate individual cells. As such, overall Iba-1 fluorescent intensity was measured to quantify microglia activation in the ME.

2.8 Flow Cytometry

12 hrs after 500 ng ICV LPS administration, mice were anesthetized using a ketamine/xylazine/acetapromide cocktail and perfused with 15 mL ice cold 0.01 M PBS to remove circulating leukocytes. After perfusion, brains were extracted and minced in a digestion solution containing 1 mg/mL type II collagenase (Sigma) and 1% DNAse (Sigma) in RPMI, then placed in a 37°C incubator for 1 hr. After digestion, myelin was removed via using 30% percoll in RPMI. Isolated cells were washed with RPMI, incubated in Fc block for 5 min, then stained with the following antibodies (all rat anti-mouse from BioLegend, except for Live/Dead) (BioLegend, San Diego, CA): anti-CD45 PerCP/Cy5.5 (1:400), anti-CD11b APC (1:800), anti-Ly6C PerCP (1:100), anti-Ly6G PE/Cy7 (1:800), anti-CD3 PE (1:100), and Live/Dead fixable aqua (1:200, Thermofisher). Flow cytometry was conducted using a Fortessa analytic flow cytometer (BD Biosciences, NJ), and analysis was performed on FlowJo V10 software (FlowJo, Ashland, OR). Cells were gated on LD, SSC singlet, and FSC singlet (Fig. 3 – figure supplement 1). Leukocytes were then defined as CD45+ cells and identified as either peripheral myeloid cells ($CD45^{high}CD11b+$) or lymphocytes ($CD45^{high}$ CD11b−). From peripheral myeloid cells $Ly6C^{low}$ monocytes ($Ly6C^{low}Ly6G-$), $Ly6C^{high}$ monocytes ($Ly6C^{high}Ly6G-$), and neutrophils ($Ly6C^{mid}$ Ly6G+) were identified. From lymphocytes, CD3+ cells were identified as T-cells.

2.9 KPC Cancer Cachexia Model

Our lab generated a mouse model of pancreatic ductal adenocarcinoma (PDAC) – associated cachexia by injection of murine-derived KPC PDAC cells (originally provided by Dr. Elizabeth Jaffee from Johns Hopkins) (Michaelis et al. 2017). These cells are derived from tumors in mice with $\underline{K}RAS^{G12D}$ and $TP\underline{5}3^{R172H}$ deleted via the PDX-1-$\underline{C}$re driver (Foley et al. 2015). Cells were maintained in RPMI supplemented with 10% heat-inactivated FBS, and 50 U/mL penicillin/streptomycin (Gibco, Thermofisher, Waltham, MA), in incubators maintained at 37°C and 5% CO_2. In the week prior to tumor implantation, animals were

transitioned to individual housing to acclimate to experimental conditions. Animal food intake and body weight were measured once daily. Mice were inoculated orthotopically with 3 million KPC tumor cells in 40 μL PBS into the tail of the pancreas (Chai et al. 2013). Sham-operated animals received heat-killed cells in the same volume. Nuclear Magnetic Resonance (NMR) measurements were taken at the beginning of the study for covariate adaptive randomization of tumor and sham groups to ensure equally distributed weight and body composition. Voluntary home cage locomotor activity was measured via MiniMitter tracking devices (Starr Life Sciences, Oakmont, PA). We only analyzed dark phase activity, based on the nocturnal nature of mice (Bains et al. 2017) and our previous studies that revealed little activity during the light phase (Michaelis et al. 2017), most of which was likely caused by humans entering the room. Mice were implanted 7 days prior to tumor implantation with MiniMitter transponders in the intrascapular subcutaneous space. Using these devices, movement counts in *x*-axis, *y*-axis, and *z*-axis were recorded in 5 min intervals. Bedding was sifted daily for any chow that may have fell to the cage floor. At 10 days post inoculation, a point when animals consistently develop cachexia (Michaelis et al. 2017), animals were euthanized, and tissues were extracted for analysis.

2.10 Statistical Analysis

Data are expressed as means ± SEM. Statistical analysis was performed with Prism 7.0 software (Graphpad Software Corp, La Jolla, CA). All data were analyzed with Two-way ANOVA analysis. For single time point experiments, the two factors in ANOVA analysis were genotype (WT vs TRIFKO in all experiments) or treatment (Saline vs LPS in Figs 1–4 or Sham vs Tumor in Fig 5). In repeated measures experiments (time course experiments – Figs 2A and B, 3A and B, 5A and C), the two factors were group and time. Main effects of genotype, treatment, group, time, and/or interaction were first analyzed, and if one effect was significant, *Bonferroni* post hoc analysis was then performed. For all analyses, significance was assigned at the level of $p < 0.05$.

3. Results

3.1 MyD88KO mice experience hypothalamic inflammation after systemic LPS challenge

Based on our previous work showing that MyD88KO mice still show subtle signs of sickness behavior after systemic LPS challenge (slight anorexia, muscle catabolism, and induction of catabolic genes) (Braun et al. 2013), we hypothesized that hypothalamic inflammation also occurred in these mice. We found that 6 hrs after 250 μg/kg IP LPS, MyD88KO mice showed increased expression of several cytokine and chemokine genes in the hypothalamus, including *Il1β*, *Tnf*, *Il6*, *Ifnβ*, *Ccl2*, *Ccl5*, *Cxcl1*, *Cxcl2*, and *Cxcl10* (Fig. 1) (Two way ANOVA treatment effect all at least $p<0.001$, post hoc analysis of MyD88KO saline vs. MyD88KO LPS all at least $p<0.01$). While upregulated in LPS-treated WT mice, *Cd80* was not significantly upregulated in LPS-treated MyD88KO mice (treatment $F_{1,12} = 23.28$, $p<0.001$; genotype $F_{1,12} = 15.14$, $p=0.002$; interaction $F_{1,12} = 19.16$, $p<0.001$. WT saline vs. WT LPS $p<0.001$, MyD88KO saline vs. MyD88KO LPS $p>0.99$ in post hoc analysis). It is important to note that the vast majority of LPS-induced cytokine and chemokine gene upregulation in the hypothalamus was attenuated in MyD88KO mice. Interestingly, *Ifnβ* only showed a slight non-significant increase in LPS-treated WT mice

compared to saline-treated WT mice, yet showed a 3.9-fold upregulation in LPS-treated MyD88KO mice compared to saline-treated MyD88KO mice (treatment effect F1,12=8.83, p=0.01, WT saline vs. WT LPS p=0.75. MyD88KO saline vs. MyD88KO LPS p=0.01 in post hoc analysis). Basal expression of all cytokines/chemokines was detectable in hypothalami of saline-treated animals.

3.2 Mice lacking TRIF show attenuated acute illness response after systemic LPS challenge

Since MyD88KO mice still show sickness behavior and hypothalamic inflammation after systemic LPS challenge, we hypothesized that other inflammatory signaling pathways are important for TLR4-driven sickness behavior. TRIF is an important adaptor protein for innate immune activation (Yamamoto et al. 2003), yet its role in sickness behavior after LPS challenge is unknown. After systemic LPS challenge (250 μg/kg, IP), TRIFKO mice showed attenuated anorexia (group effect $F_{3,140} = 312.9$, $p<0.001$, post hoc analysis of WT LPS vs. TRIFKO LPS at least $p<0.001$ every time point after LPS injection) and weight loss (group effect $F_{3,100} = 431.7$, $p<0.001$, post hoc analysis of WT LPS vs. TRIFKO LPS at least $p<0.01$ starting 6 hrs after LPS injection) compared to WT mice (Fig. 2A and B). Next, in order to determine the degree of hypothalamic activation and quantify acute stress response, we measured plasma corticosterone (Gong et al. 2015). While WT mice showed a large increase in plasma corticosterone 4 hrs after IP LPS administration ($p<0.001$), LPS-treated TRIFKO mice did not show a significant increase (interaction effect $F_{1,18} = 19.79$, $p<0.001$, WT saline vs. WT LPS $p<0.01$, TRIFKO saline vs. TRIFKO LPS $p = 0.06$ in post hoc analysis)(Fig. 2C).

CNS inflammation is a hallmark of acute illness responses and cachexia. Therefore, we measured expression of inflammatory cytokine and chemokine genes in the hypothalamus after systemic LPS challenge using qRT-PCR. We found that 6 hrs after 250 μg/kg IP LPS, TRIFKO animals showed attenuated up-regulation of several cytokines and chemokines in the hypothalamus, including *Il6*, *Ccl2*, *Ccl5*, *Cxcl1*, *Cxcl2*, and *Cxcl10* (interaction effect at least $p<0.05$) (Fig. 2D). Alternatively, *Il1β*, *Tnf* were not differentially upregulated in LPS-treated TRIFKO mice compared to WT LPS-treated mice (treatment effect $p<0.05$, and post hoc analysis comparing saline to LPS-treatment within the same genotype $p<0.05$, but interaction effect $p>0.05$ for both). In contrast to Figure 1, we did not observe a treatment effect of LPS on WT mice for *Cd80* (treatment effect $F_{1,12} = 0.68$, $p=0.43$), yet did see an interaction effect ($F_{1,12} = 6.57$, $p=0.02$). Lastly, we did not observe any treatment ($F_{1,12} = 0.726$, $p=0.411$), genotype ($F_{1,12} = 0.346$, $p=0.567$), or interaction ($F_{1,12}<0.001$, $p=0.995$) effect in our analysis of *Ifnβ* expression in the hypothalamus. It is important to note that basal expression of all cytokines/chemokines was detectable in hypothalami of saline-treated animals.

In order to rule out altered MyD88 signaling as a result of TRIF deletion, we challenged TRIFKO mice with 10 ng ICV IL-1β. MyD88 is essential for IL-1R signaling, but TRIF is not involved (Muzio et al. 1997). We found that WT and TRIFKO mice had similar anorexia response to ICV IL-1β (Fig. S1A). While WT IL-1β-treated mice lost more weight than WT saline-treated mice, it was not significantly more than TRIFKO IL-1β-treated mice. Lastly,

Myd88 was equally expressed in WT and TRIFKO mice at baseline, and similarly upregulated after IP LPS exposure (Fig. S1C).

3.3 TRIF is important in acute illness response after ICV LPS challenge

To determine the role of TRIF signaling in the CNS after TLR4 activation, we injected LPS directly into the brain lateral ventricles of WT and TRIFKO mice at a dose that has no behavioral effects when injected peripherally (50 ng). Two-way ANOVA analysis revealed a significant group effect after ICV injection of 50 ng LPS ($F_{3,126} = 313.4$, $p<0.001$). Subsequent post hoc *analysis* showed that while LPS caused a significant decrease in cumulative food intake in both WT and TRIFKO animals, starting 36 hrs after treatment TRIFKO animals consumed more than WT animals (p at least <0.01) (Fig. 3A). We found similar results when comparing body weight after ICV LPS treatment. Two-way ANOVA analysis revealed a significant group effect after ICV injection of 50 ng LPS ($F_{3,90} = 103.2$, $p<0.001$), and subsequent post hoc analysis showed that TRIFKO mice treated with ICV LPS experienced significantly attenuated weight loss compared to WT mice treated with ICV LPS at 24 and 36 hrs after injection (p at least <0.01)(Fig. 3B).

3.4 TRIF is required for microglial activation after ICV LPS treatment

TRIF is important for microglia function during states of disease (Hosmane et al. 2012). However, no studies have investigated the role of TRIF in microglial activation after TLR4 stimulation. Therefore, we quantified microglial activation in the MBH 12 hrs after ICV LPS administration (50 ng) by measuring Iba-1 intensity per cell and cell area. While arcuate nucleus microglia in LPS-treated WT mice showed a significant increase in size compared to saline-treated WT, arcuate nucleus microglia in LPS-treated TRIFKO mice did not increase in size compared to saline-treated TRIFKO mice (treatment effect $F_{1,12} = 16.73$, $p = 0.0015$, WT saline vs. WT LPS $p<0.01$, TRIFKO saline vs. TRIFKO LPS $p = 0.32$ in post hoc analysis) (Fig. 3E). In the arcuate nucleus, Iba-1 intensity per microglia did not increase in the LPS-treated group for either genotype (Fig. 3F). However, overall Iba-1 intensity increased in the median eminence in the WT LPS-treated group compared to the WT saline-treated group, but not in the TRIFKO LPS-treated group compared to the TRIFKO saline-treated group (treatment effect $F_{1,12} = 8.82$, $p = 0.02$, WT saline vs. WT LPS $p<0.05$, TRIFKO saline vs. TRIFKO LPS $p>0.99$ in post hoc analysis) (Fig. 3G).

3.5 TRIF is required for neutrophil recruitment to the brain

Since chemokines comprised the majority of inflammatory transcripts that were less upregulated in TRIFKO mice after LPS exposure, we hypothesized that TRIF is important in immune cell recruitment to the brain. We performed flow cytometry on the brains of WT and TRIFKO mice 12 hrs after 500 ng ICV LPS exposure. We focused our analysis on neutrophils based on previous literature showing they are the predominant cell type in the brain after LPS exposure (He et al. 2016). We found that, compared to saline-treated WT mice, LPS-treated WT mice had a significantly higher percentage of CD45+ cells in the brain that were neutrophils (treatment effect $F_{1,12} = 18.69$, $p = 0.001$, WT saline vs. WT LPS $p = 0.0028$ in post hoc analysis) (Fig. 4C). Alternatively, compared to saline-treated TRIFKO mice, LPS-treated TRIFKO mice did not have an increased percentage of CD45+ cells in the brain that were neutrophils (TRIFKO saline vs. TRIFKO LPS $p = 0.14$) (Fig.

4C). In WT animals there was a decrease in percentage of CD45+ cells that were T-cells (treatment effect F1,12 = 8.15, p=0.0145, WT saline vs WT LPS p = 0.019 in post hoc analysis). There was no change in $Ly6C^{low}$, or $Ly6C^{high}$ monocytes after LPS exposure in either genotype (treatment, genotype, and interaction all p>0.05 in Two-way ANOVA) (Fig. 4D).

3.6 Mice lacking TRIF have attenuated cancer cachexia

TRIFKO mice inoculated orthotopically with KPC PDAC cells experienced attenuated anorexia compared to WT mice with PDAC (Fig. 5A and B). Furthermore, TRIFKO tumor mice showed attenuated voluntary locomotor activity (LMA) compared to WT tumor mice, as defined by dark cycle home cage activity (Grossberg et al. 2011; Gabriel Knoll, Krasnow, and Marks 2017) (Fig. 5C). While Two-way ANOVA analysis of dark cycle LMA days 3–10 (time from which cachexia response was initiated) revealed a significant group effect (F3, 128 = 45.75, p<0.001), no post hoc comparisons between the WT tumor and TRIFKO tumor group were significant. However, when Three-way ANOVA analysis was performed (analyzing the effects of tumor status, genotype, and time), the interaction between genotype and tumor status was significant (F = 4.35, df 1,128, p = 0.035). WT tumor-bearing mice showed significantly decreased gastrocnemius mass compared to WT sham-operated mice (Two-way ANOVA treatment effect F1,16 = 5.064, p = 0.039, WT sham vs. WT tumor p = 0.022 in post hoc analysis) while TRIFKO tumor-bearing mice did not show decreased gastrocnemius mass compared to TRIFKO sham-operated mice (p>0.99) (Fig. 5D). These effects on muscle catabolism were further evidenced by the fact that the E3 ubiquitin-ligase system genes *Mafbx* and *Murf1* were upregulated in WT tumor animals compared to WT sham animals (treatment effect p<0.001 for all three, post hoc analysis all at least p<0.01), but not significantly upregulated in TRIFKO tumor-bearing animals (interaction effect at least p<0.05)(Fig. 5E). The same was true for *Foxo1*, a key transcription factor for muscle catabolism (Sandri et al. 2004). In addition, although *Ccl2* was significantly upregulated in the hypothalamus of WT tumor animals compared to sham animals (treatment effect p<0.01), it was not in TRIFKO tumor-bearing animals (interaction effect p<0.05). Alternatively, compared to WT tumor-bearing animals, *Il1β* was equally upregulated in the hypothalami of TRIFKO tumor-bearing animals (treatment effect p<0.05, but interaction effect p>0.05), and *Tnf*, *Il6*, *Cd80*, *Cxcl1*, *Cxcl2*, and *Cxcl10* were not upregulated in the hypothalami WT or TRIFKO tumor-bearing animals. Lastly, although *Ccl5* was less upregulated in the hypothalami of TRIFKO tumor-bearing animals compared to WT tumor-bearing animals, this relationship was not significant (interaction effect F1,16 = 1.339, p>0.05)(Fig. 5F).

4. Discussion

We investigated the role of TRIF in acute sickness behavior after LPS exposure and in a model of pancreatic cancer cachexia. These studies demonstrated that TRIFKO mice experienced attenuated sickness behavior after peripheral or central LPS exposure. Furthermore, TRIFKO mice experienced attenuated cachexia during PDAC, including decreased anorexia, voluntary LMA, muscle catabolism, and hypothalamic inflammation relative to WT counterparts. These results indicate that TRIF is an important mediator of

inflammation-driven sickness behavior, and should be considered during the development of anti-inflammatory therapies for cachexia.

Several studies investigated the role of MyD88 in sickness behavior (Yamawaki et al. 2010; Braun et al. 2012; Zhu et al. 2016), yet evidence suggests that MyD88-independent signaling pathways are important in CNS immune activation (Hosmane et al. 2012; Menasria et al. 2013). We found that MyD88KO mice still experienced hypothalamic inflammation. It is important to note that while many inflammatory cytokine and chemokine genes were upregulated in LPS-treated MyD88KO mice compared to saline-treated MyD88KO mice, the expression of genes in the LPS-treated MyD88KO mice was much lower than that in LPS-treated WT animals. This shows that MyD88 is a key mediator of LPS-induced neuroinflammation, but there are other mediators important in inflammatory gene expression.

While the role of TRIF signaling in acute sickness behavior during viral infection was investigated previously (Zhu et al. 2016; Murray et al. 2015; Gibney et al. 2013), these studies focused on the effects of a single injection of Poly I:C, a viral double-stranded RNA mimetic, on acute sickness behavior and neuroinflammation. Poly I:C is a known TLR3 agonist and is a model of acute viral illness. Alternatively, this is the first study to investigate the role of TRIF in acute sickness behavior after LPS exposure and during cachexia. After systemic challenge with LPS, TRIFKO mice experienced attenuated anorexia and weight loss compared to WT mice. These results also coincided with an attenuated increase in serum corticosterone, implicating TRIF as a key player in stress response. Furthermore, LPS-treated TRIFKO mice showed attenuated hypothalamic inflammation compared to WT mice. Interestingly, we found that *Ifnβ*, a key transcript regulated by TRIF signaling, was not induced by LPS exposure or cancer in WT or TRIFKO mice. To our knowledge, this is the first report of *Ifnβ* gene expression in the hypothalamus after systemic LPS exposure. It is possible *Ifn*β was induced earlier than 6 hrs after LPS exposure, since it was previously shown that *Ifn*β mRNA is upregulated in the hippocampus 2 hrs after 100 μg/kg IP LPS (Skelly et al. 2013). Future studies should investigate the expression of type I interferons in the hypothalamus at different time points after LPS exposure.

In addition to attenuated acute sickness behavior after systemic LPS exposure, TRIFKO mice experienced attenuated anorexia and weight loss after ICV LPS administration. Interestingly, TRIFKO mice showed similar weight loss 12 hours after LPS administration, yet recovered more rapidly than WT mice, reaching baseline body weight 36 hours after injection. While it has been previously reported that TLR4 is important in neuroinflammation and acute sickness behavior after IP LPS exposure (Hines et al. 2013), the kinetics of different signaling pathways linked to TLR4 are not known. Our results suggest that in the CNS, MyD88 may drive initial sickness response after TLR4 activation, whereas TRIF signaling may be involved in maintaining inflammation and subsequent sickness response. It should be noted that a repeated measures three-way ANOVA would provide valuable information on the interaction between time, genotype, and treatment status. Unfortunately, our experiments were not sufficiently powered for this analysis. Future studies should investigate the kinetics of TRIF-dependent acute sickness behavior in detail.

In the brain, microglia express TRIF at basal levels, and this expression is enhanced by various CNS insults (Lin et al. 2012; Wang et al. 2013). Review of the published online database (https://web.stanford.edu/group/barres_lab/brain_rnaseq.html) confirms that the basal expression of TRIF (*Ticam1*) is predominantly found in microglia (Zhang et al. 2014). We found that, unlike in WT mice, microglia in TRIFKO mice did not show an increase in Iba-1 intensity in the ME or an increase in Iba-1+ cell size in the ARC 12 hrs after ICV LPS administration. While additional studies are needed to characterize the functional changes in TRIFKO microglia after LPS exposure, these results are in agreement with previous studies showing that TRIF expression in microglia is required for normal inflammatory activation and phagocytosis in response to neuronal injury (Hosmane et al. 2012; Lin et al. 2012). Furthermore, in a murine model of intracerebral hemorrhage, TRIFKO mice showed attenuated neurologic disability and neuroinflammation. In addition, TLR2 activation in hypothalamic microglia was shown to generate sickness responses (Jin et al. 2016). TRIF is now known to be linked to TLR2 signaling (Nilsen et al. 2015; Petnicki-Ocwieja et al. 2013). Therefore, our data, in addition to previous findings, suggest TRIF is important in microglial activation during states of inflammation, which is important in driving subsequent functional and behavioral response.

We found that TRIFKO mice experienced attenuated hypothalamic inflammation after systemic LPS exposure. Interestingly, amongst the differentially regulated transcripts between WT and TRIFKO animals, there was a predominance of chemokine mRNAs (*Ccl2*, *Ccl5*, *Cxcl1*, *Cxcl10*). Previous studies showed that acute LPS exposure results in peripheral immune cell recruitment to the brain (He et al. 2016) and that infiltrating immune cells in the brain drive sickness behavior in states of chronic inflammation (D'Mello, Le, and Swain 2009). Based on these data, we investigated whether TRIFKO mice had decreased immune cell infiltration into the brain after ICV LPS exposure and found that TRIF was required for neutrophil recruitment. Interestingly, we did see a nonsignificant increase in Ly6Chi monocytes. While it is difficult to speculate on trends, it is possible there was a compensatory increase in the cells as a result of TRIF deletion causing an altered inflammatory reaction. While TRIF is known to be important for neutrophil recruitment to the lungs (Liu et al. 2016), this is the first study to implicate TRIF in neutrophil recruitment to the brain. This presents a novel mechanism that can be applied to several pathologies, including CNS infection, cancer, and stroke. Furthermore, while neutrophils may appear after the onset of initial sickness behaviors in the setting of acute illness, no studies have investigated whether neutrophils are important in sickness behavior or cachexia. In addition, it is important to note that while our flow cytometry results cannot distinguish if the CNS neutrophils have translocated into the brain parenchyma, several lines of evidence demonstrate that adherent intravascular neutrophils contribute to inflammation and pathology in the brain (Atangana et al. 2017; Ruhnau et al. 2017). Interestingly, brain-infiltrating neutrophils in LPS-treated TRIFKO mice showed a nonsignificant increase in Ly6G expression compared to brain-infiltrating neutrophils in LPS-treated WT mice, sometimes so much so that the Ly6G expression exceeded the pre-defined “maximum” fluorescent intensity. This suggests that brain-infiltrating neutrophils in TRIFKO mice may have a different phenotype than those in WT mice. More advanced flow cytometry studies

(intracellular staining for cytokines and enzymes) and histology studies are needed to further investigate this observation.

When inflammation is maintained, acute sickness behavior transforms into cachexia, a maladaptive condition associated with increased mortality and decreased quality of life during numerous chronic diseases (Bachmann et al. 2008; Wesseltoft-Rao et al. 2015; Lainscak, Podbregar, and Anker 2007). While inflammation is critical for cachexia, mechanisms of inflammatory signaling important for this syndrome remain unclear. We found that in a mouse model of PDAC-associated cachexia, TRIFKO mice experienced attenuated anorexia, voluntary LMA, muscle catabolism, and hypothalamic inflammation compared to WT mice. While our results were consistent across various behavioral and molecular measures of cachexia, it is important to note that the effects of *Ticam1* deletion were modest. It is important to note that differences in dark cycle home cage LMA between WT tumor and TRIFKO tumor were significant only when analysis was expanded to Three-way ANOVA, a testament to the minor effects of TRIF on this measure of cachexia. These results suggest that other inflammatory signaling pathways are important in cachexia. Rudd et al. previously reported that MyD88KO mice were resistant to anorexia in a methylcholanthrene-induced sarcoma tumor model (Ruud et al. 2010). However, this was a short report and their analysis of cachexia was limited to food intake and carcass weight.

The main limitation of the present study is the lack of cell specificity in global TRIFKO experiments. Future studies are needed to identify the critical cell type involved in TRIF-mediated sickness behavior and cachexia. Furthermore, we only assessed muscle catabolism only in the gastrocnemius. While gastrocnemius may not be representative of all skeletal muscle, we previously reported that other muscle groups (tibialis anterior, soleus, etc.) showed similar catabolic changes during PDAC cachexia (Michaelis et al. 2017). In addition, we only used a single measure of stress response (circulating corticosterone levels 4 hrs after LPS exposure). While a single test is not sufficient to fully define the role of TRIF in stress response, previous studies have shown 4 hr circulating corticosterone levels as a robust measure of acute stress response (Pérez-Nievas et al. 2010; Johnson, Propes, and Shavit 1996). In addition, we report results from multiple experiments using different doses ICV LPS administration. We chose a dose sufficient to induce sickness response when injected centrally, but not when injected peripherally (50 ng), and the smallest single dose required to induce neutrophil recruitment to the brain (500 ng, data not shown). While whether or not LPS crosses the blood brain barrier (BBB) remains controversial (Banks and Robinson 2010), we believe this route of administration is sufficient for the purpose of this study for two reasons. First, the MBH contains a dramatically attenuated BBB, allowing circulating molecules to access the parenchyma in the region (Rodríguez, Blázquez, and Guerra 2010; Morita and Miyata 2013). Second, there are several ways that peripherally administered LPS induces neuroinflammation (acute phase response proteins, platelet mobilization, peripheral immune cell-derived cytokines, vagus nerve activation, etc.) (de Stoppelaar et al. 2014; Le Thuc et al. 2017). Therefore, we chose to make many of our observations with low-dose LPS delivered centrally to minimize confounders. Another limitation is the fact that we performed analysis of cachexia using only one mouse model of cancer cachexia. Caution is warranted when applying our results to other types of cachexia (heart failure, cirrhosis, untreated HIV, other types of cancer, etc.). However, this model is

extensively characterized (Michaelis et al. 2017), and recapitulates all of the cardinal features of cachexia seen in humans. Furthermore, it avoids many of the shortcomings in other mouse models of cachexia, including: multiple clones with variable cachexia (Kir et al. 2014), cachexia driven by only a single cytokine (Talbert et al. 2014), and requiring advanced surgical techniques to induce cachexia (DeBoer 2009). Nevertheless, future studies should assess the effects of *Ticam1* deletion in other models of cachexia, as well as the tumor immune response in TRIFKO mice.

In conclusion, we report that TRIF is important in acute sickness behavior and cachexia. These results show that TRIF-dependent mechanisms should be considered when developing therapeutic targets for cachexia. Future studies are needed to identify the important cell types involved in TRIF signaling during acute illness response and cachexia.

Supplementary Material

Refer to Web version on PubMed Central for supplementary material.

Acknowledgments

We would like to thank Dr. James Friedrich for his assistance with statistical analysis. This work was supported by the National Institutes of Health (grant number 1 R01 CA184324-01, DLM) and the Brendan-Colson Center for Pancreatic Care.

References

Anker SD, Ponikowski P, Varney S, Chua TP, Clark AL, Webb-Peploe KM, Harrington D, Kox WJ, Poole-Wilson PA, Coats AJ. Wasting as independent risk factor for mortality in chronic heart failure. Lancet. 1997; 349:1050–3. [PubMed: 9107242]

Argiles JM, Anker SD, Evans WJ, Morley JE, Fearon KC, Strasser F, Muscaritoli M, Baracos VE. Consensus on cachexia definitions. J Am Med Dir Assoc. 2010; 11:229–30. [PubMed: 20439040]

Atangana E, Schneider UC, Blecharz K, Magrini S, Wagner J, Nieminen-Kelha M, Kremenetskaia I, Heppner FL, Engelhardt B, Vajkoczy P. Intravascular Inflammation Triggers Intracerebral Activated Microglia and Contributes to Secondary Brain Injury After Experimental Subarachnoid Hemorrhage (eSAH). Transl Stroke Res. 2017; 8:144–56. [PubMed: 27477569]

Bachmann J, Heiligensetzer M, Krakowski-Roosen H, Buchler MW, Friess H, Martignoni ME. Cachexia worsens prognosis in patients with resectable pancreatic cancer. J Gastrointest Surg. 2008; 12:1193–201. [PubMed: 18347879]

Bains Rasneer S, Wells SaraSillito Rowland R, Armstrong J DouglasCater Heather L, Banks GarethNolan Patrick M. Assessing mouse behaviour throughout the light/dark cycle using automated in-cage analysis tools. Journal of Neuroscience Methods. 2017

Banks William A, Robinson Sandra M. Minimal Penetration of Lipopolysaccharide Across the Murine Blood-brain Barrier. Brain Behav Immun. 2010; 24:102–09. [PubMed: 19735725]

Bluthé Rose-MarieMichaud BrunoPoli ValeriaDantzer Robert. Role of IL-6 in cytokine-induced sickness behavior: a study with IL-6 deficient mice. Physiol Behav. 2000; 70:367–73. [PubMed: 11006436]

Bodnar RJ, Pasternak GW, Mann PE, Paul D, Warren R, Donner DB. Mediation of anorexia by human recombinant tumor necrosis factor through a peripheral action in the rat. Cancer Res. 1989; 49:6280–4. [PubMed: 2804974]

Braun TP, Grossberg AJ, Veleva-Rotse BO, Maxson JE, Szumowski M, Barnes AP, Marks DL. Expression of myeloid differentiation factor 88 in neurons is not requisite for the induction of sickness behavior by interleukin-1beta. J Neuroinflammation. 2012; 9:229. [PubMed: 23031643]

Braun TP, Zhu X, Szumowski M, Scott GD, Grossberg AJ, Levasseur PR, Graham K, Khan S, Damaraju S, Colmers WF, Baracos VE, Marks DL. Central nervous system inflammation induces muscle atrophy via activation of the hypothalamic-pituitary-adrenal axis. J Exp Med. 2011; 208:2449–63. [PubMed: 22084407]

Braun Theodore P, Grossberg Aaron J, Krasnow Stephanie M, Levasseur Peter R, Szumowski MarekZhu Xin XiaMaxson Julia E, Knoll J GabrielBarnes Anthony P, Marks Daniel L. Cancer- and endotoxin-induced cachexia require intact glucocorticoid signaling in skeletal muscle. The FASEB Journal. 2013; 27:3572–82. [PubMed: 23733748]

Burfeind KG, Michaelis KA, Marks DL. The central role of hypothalamic inflammation in the acute illness response and cachexia. Semin Cell Dev Biol. 2015

Chai MG, Kim-Fuchs C, Angst E, Sloan EK. Bioluminescent orthotopic model of pancreatic cancer progression. J Vis Exp. 2013

D'Mello C, Le T, Swain MG. Cerebral microglia recruit monocytes into the brain in response to tumor necrosis factoralpha signaling during peripheral organ inflammation. J Neurosci. 2009; 29:2089–102. [PubMed: 19228962]

Dantzer RobertBluthÉ Rose-MarieLayÉ SophieBret-Dibat Jean-LucParnet PatriciaKelley Keith W. Cytokines and Sickness Behavior. Ann N Y Acad Sci. 1998; 840:586–90. [PubMed: 9629285]

de Stoppelaar Sacha F, van 't Veer CornelisClaushuis Theodora AM, Albersen Bregje JA, Roelofs Joris JTH, van der Poll Tom. Thrombocytopenia impairs host defense in gram-negative pneumonia–derived sepsis in mice. Blood. 2014; 124:3781–90. [PubMed: 25301709]

DeBoer Mark Daniel. Animal models of anorexia and cachexia. Expert opinion on drug discovery. 2009; 4:1145–55. [PubMed: 20160874]

Elmquist JK, Scammell TE, Jacobsen CD, Saper CB. Distribution of Fos-like immunoreactivity in the rat brain following intravenous lipopolysaccharide administration. J Comp Neurol. 1996; 371:85–103. [PubMed: 8835720]

Evans WJ, Morley JE, Argiles J, Bales C, Baracos V, Guttridge D, Jatoi A, Kalantar-Zadeh K, Lochs H, Mantovani G, Marks D, Mitch WE, Muscaritoli M, Najand A, Ponikowski P, Rossi Fanelli F, Schambelan M, Schols A, Schuster M, Thomas D, Wolfe R, Anker SD. Cachexia: a new definition. Clin Nutr. 2008; 27:793–9. [PubMed: 18718696]

Fearon K, Strasser F, Anker SD, Bosaeus I, Bruera E, Fainsinger RL, Jatoi A, Loprinzi C, MacDonald N, Mantovani G, Davis M, Muscaritoli M, Ottery F, Radbruch L, Ravasco P, Walsh D, Wilcock A, Kaasa S, Baracos VE. Definition and classification of cancer cachexia: an international consensus. Lancet Oncol. 2011; 12:489–95. [PubMed: 21296615]

Feng Y, Zou L, Zhang M, Li Y, Chen C, Chao W. MyD88 and Trif signaling play distinct roles in cardiac dysfunction and mortality during endotoxin shock and polymicrobial sepsis. Anesthesiology. 2011; 115:555–67. [PubMed: 21792053]

Foley K, Rucki AA, Xiao Q, Zhou D, Leubner A, Mo G, Kleponis J, Wu AA, Sharma R, Jiang Q, Anders RA, Iacobuzio-Donahue CA, Hajjar KA, Maitra A, Jaffee EM, Zheng L. Semaphorin 3D autocrine signaling mediates the metastatic role of annexin A2 in pancreatic cancer. Sci Signal. 2015; 8:ra77. [PubMed: 26243191]

Gabriel Knoll J, Krasnow Stephanie M, Marks Daniel L. Interleukin-1β signaling in fenestrated capillaries is sufficient to trigger sickness responses in mice. J Neuroinflammation. 2017; 14:219. [PubMed: 29121947]

Gibney Sinead M, McGuinness BarryPrendergast ChristineHarkin AndrewConnor Thomas J. Poly I: C-induced activation of the immune response is accompanied by depression and anxiety-like behaviours, kynurenine pathway activation and reduced BDNF expression. Brain Behav Immun. 2013; 28:170–81. [PubMed: 23201589]

Gong ShuaiMiao Yi-LongJiao Guang-ZhongSun Ming-JuLi HongLin JuanLuo Ming-JiuTan Jing-He. Dynamics and Correlation of Serum Cortisol and Corticosterone under Different Physiological or Stressful Conditions in Mice. PLoS One. 2015; 10:e0117503. [PubMed: 25699675]

Grossberg Aaron J, Zhu XinXiaLeinninger Gina M, Levasseur Peter R, Braun Theodore P, Myers Martin G, Marks Daniel L. Inflammation-induced lethargy is mediated by suppression of orexin neuron activity. J Neurosci. 2011; 31:11376–86. [PubMed: 21813697]

Hanke Mark L, Kielian Tammy. Toll-like receptors in health and disease in the brain: mechanisms and therapeutic potential. Clinical science (London, England : 1979). 2011; 121:367–87.

He HaoGeng TingtingChen PiyunWang MeixiangHu JingxiaKang LiSong WengangTang Hua. NK cells promote neutrophil recruitment in the brain during sepsis-induced neuroinflammation. Scientific Reports. 2016; 6:27711. [PubMed: 27270556]

Hines Dustin J, Choi Hyun B, Hines Rochelle M, Phillips Anthony G, MacVicar Brian A. Prevention of LPS-Induced Microglia Activation, Cytokine Production and Sickness Behavior with TLR4 Receptor Interfering Peptides. PLoS One. 2013; 8:e60388. [PubMed: 23555964]

Hosmane SuneilTegenge Million AdaneRajbhandari LabchanUapinyoying PrechKumar Nishant GaneshThakor NitishVenkatesan Arun. TRIF mediates microglial phagocytosis of degenerating axons. The Journal of Neuroscience. 2012; 32:7745–57. [PubMed: 22649252]

Jin SunghoKim Jae GeunPark Jeong WooKoch MarcoHorvath Tamas L, Lee Byung Ju. Hypothalamic TLR2 triggers sickness behavior via a microglia-neuronal axis. Scientific Reports. 2016; 6:29424. [PubMed: 27405276]

Johnson RW, Propes MJ, Shavit Y. Corticosterone modulates behavioral and metabolic effects of lipopolysaccharide. Am J Physiol. 1996; 270:R192–8. [PubMed: 8769802]

Kir S, White JP, Kleiner S, Kazak L, Cohen P, Baracos VE, Spiegelman BM. Tumour-derived PTH-related protein triggers adipose tissue browning and cancer cachexia. Nature. 2014; 513:100–4. [PubMed: 25043053]

Konsman JP, Tridon V, Dantzer R. Diffusion and action of intracerebroventricularly injected interleukin-1 in the CNS. Neuroscience. 2000; 101:957–67. [PubMed: 11113345]

Kotler DP, Tierney AR, Wang J, Pierson RN Jr. Magnitude of body-cell-mass depletion and the timing of death from wasting in AIDS. Am. J. Clin. Nutr. 1989; 50:444–47. [PubMed: 2773823]

Laflamme N, Rivest S. Effects of systemic immunogenic insults and circulating proinflammatory cytokines on the transcription of the inhibitory factor kappaB alpha within specific cellular populations of the rat brain. J Neurochem. 1999; 73:309–21. [PubMed: 10386984]

Lainscak M, Podbregar M, Anker SD. How does cachexia influence survival in cancer, heart failure and other chronic diseases? Curr Opin Support Palliat Care. 2007; 1:299–305. [PubMed: 18685379]

Le Thuc O, Stobbe K, Cansell C, Nahon JL, Blondeau N, Rovere C. Hypothalamic Inflammation and Energy Balance Disruptions: Spotlight on Chemokines. Front Endocrinol (Lausanne). 2017; 8:197. [PubMed: 28855891]

Lin S, Yin Q, Zhong Q, Lv FL, Zhou Y, Li JQ, Wang JZ, Su BY, Yang QW. Heme activates TLR4-mediated inflammatory injury via MyD88/TRIF signaling pathway in intracerebral hemorrhage. J Neuroinflammation. 2012; 9:46. [PubMed: 22394415]

Liu Y, Gu Y, Han Y, Zhang Q, Jiang Z, Zhang X, Huang B, Xu X, Zheng J, Cao X. Tumor Exosomal RNAs Promote Lung Pre-metastatic Niche Formation by Activating Alveolar Epithelial TLR3 to Recruit Neutrophils. Cancer Cell. 2016; 30:243–56. [PubMed: 27505671]

Medzhitov R, Preston-Hurlburt P, Kopp E, Stadlen A, Chen C, Ghosh S, Janeway CA Jr. MyD88 is an adaptor protein in the hToll/IL-1 receptor family signaling pathways. Mol Cell. 1998; 2:253–8. [PubMed: 9734363]

Menasria R, Boivin N, Lebel M, Piret J, Gosselin J, Boivin G. Both TRIF and IPS-1 adaptor proteins contribute to the cerebral innate immune response against HSV-1 infection. J Virol. 2013

Michaelis KA, Zhu X, Burfeind KG, Krasnow SM, Levasseur PR, Morgan TK, Marks DL. Establishment and characterization of a novel murine model of pancreatic cancer cachexia. J Cachexia Sarcopenia Muscle. 2017; 8:824–38. [PubMed: 28730707]

Morgan JI, Curran T. Role of ion flux in the control of c-fos expression. Nature. 1986; 322:552–5. [PubMed: 2426600]

Morita S, Miyata S. Accessibility of low-molecular-mass molecules to the median eminence and arcuate hypothalamic nucleus of adult mouse. Cell Biochem Funct. 2013; 31:668–77. [PubMed: 23348371]

Murray CarolGriffin Éadaoin W, O'Loughlin ElaineLyons AoifeSherwin EoinAhmed SuaadStevenson Nigel J, Harkin AndrewCunningham Colm. Interdependent and independent roles of type I

interferons and IL-6 in innate immune, neuroinflammatory and sickness behaviour responses to systemic poly I:C. Brain Behav Immun. 2015; 48:274–86. [PubMed: 25900439]

Muzio M, Ni J, Feng P, Dixit VM. IRAK (Pelle) family member IRAK-2 and MyD88 as proximal mediators of IL-1 signaling. Science. 1997; 278:1612–5. [PubMed: 9374458]

Nilsen NJ, Vladimer GI, Stenvik J, Orning MP, Zeid-Kilani MV, Bugge M, Bergstroem B, Conlon J, Husebye H, Hise AG, Fitzgerald KA, Espevik T, Lien E. A role for the adaptor proteins TRAM and TRIF in toll-like receptor 2 signaling. J Biol Chem. 2015; 290:3209–22. [PubMed: 25505250]

Pérez-Nievas Beatriz G, Madrigal José LM, García-Bueno BorjaZoppi SilviaLeza Juan C. Corticosterone basal levels and vulnerability to LPS-induced neuroinflammation in the rat brain. Brain Res. 2010; 1315:159–68. [PubMed: 20026014]

Petnicki-Ocwieja TanjaChung ErinAcosta David I, Ramos Laurie T, Shin Ok S, Ghosh SanjuktaKobzik LesterLi XinHu Linden T. TRIF Mediates Toll-Like Receptor 2-Dependent Inflammatory Responses to Borrelia burgdorferi. Infect Immun. 2013; 81:402–10. [PubMed: 23166161]

Rodríguez Esteban M, Blázquez Juan L, Guerra Montserrat. The design of barriers in the hypothalamus allows the median eminence and the arcuate nucleus to enjoy private milieus: The former opens to the portal blood and the latter to the cerebrospinal fluid. Peptides. 2010; 31:757–76. [PubMed: 20093161]

Ruhnau JohannaSchulze JulianeDressel AlexanderVogelgesang Antje. Thrombosis, Neuroinflammation, and Poststroke Infection: The Multifaceted Role of Neutrophils in Stroke. Journal of Immunology Research. 2017; 2017:5140679. [PubMed: 28331857]

Ruud J, Backhed F, Engblom D, Blomqvist A. Deletion of the gene encoding MyD88 protects from anorexia in a mouse tumor model. Brain Behav Immun. 2010; 24:554–7. [PubMed: 20093176]

Sandri M, Sandri C, Gilbert A, Skurk C, Calabria E, Picard A, Walsh K, Schiaffino S, Lecker SH, Goldberg AL. Foxo transcription factors induce the atrophy-related ubiquitin ligase atrogin-1 and cause skeletal muscle atrophy. Cell. 2004; 117:399–412. [PubMed: 15109499]

Skelly Donal T, Hennessy EdelDansereau Marc-AndreCunningham Colm. A Systematic Analysis of the Peripheral and CNS Effects of Systemic LPS, IL-1B, TNF-α and IL-6 Challenges in C57BL/6 Mice. PLoS One. 2013; 8:e69123. [PubMed: 23840908]

Sonti G, Ilyin SE, Plata-Salaman CR. Anorexia induced by cytokine interactions at pathophysiological concentrations. Am J Physiol. 1996; 270:R1394–402. [PubMed: 8764309]

Talbert Erin E, Metzger Gregory A, He Wei A, Guttridge Denis C. Modeling human cancer cachexia in colon 26 tumor-bearing adult mice. Journal of Cachexia, Sarcopenia and Muscle. 2014; 5:321–28.

Tisdale MJ. Cachexia in cancer patients. Nat Rev Cancer. 2002; 2:862–71. [PubMed: 12415256]

Wang AY, Sea MM, Tang N, Sanderson JE, Lui SF, Li PK, Woo J. Resting energy expenditure and subsequent mortality risk in peritoneal dialysis patients. J Am Soc Nephrol. 2004; 15:3134–43. [PubMed: 15579517]

Wang Y, He H, Li D, Zhu W, Duan K, Le Y, Liao Y, Ou Y. The role of the TLR4 signaling pathway in cognitive deficits following surgery in aged rats. Mol Med Rep. 2013; 7:1137–42. [PubMed: 23426570]

Wesseltoft-Rao N, Hjermstad MJ, Ikdahl T, Dajani O, Ulven SM, Iversen PO, Bye A. Comparing two classifications of cancer cachexia and their association with survival in patients with unresected pancreatic cancer. Nutr Cancer. 2015; 67:472–80. [PubMed: 25710201]

Wisse BE, Ogimoto K, Tang J, Harris MK Jr, Raines EW, Schwartz MW. Evidence that lipopolysaccharide-induced anorexia depends upon central, rather than peripheral, inflammatory signals. Endocrinology. 2007; 148:5230–7. [PubMed: 17673516]

Yamamoto M, Sato S, Hemmi H, Hoshino K, Kaisho T, Sanjo H, Takeuchi O, Sugiyama M, Okabe M, Takeda K, Akira S. Role of adaptor TRIF in the MyD88-independent toll-like receptor signaling pathway. Science. 2003; 301:640–3. [PubMed: 12855817]

Yamawaki YosukeKimura HitomiHosoi ToruOzawa Koichiro. MyD88 plays a key role in LPS-induced Stat3 activation in the hypothalamus. American Journal of Physiology - Regulatory, Integrative and Comparative Physiology. 2010; 298:R403.

Zhang YeChen KenianSloan Steven A, Bennett Mariko L, Scholze Anja R, O'Keeffe SeanPhatnani Hemali P, Guarnieri PaoloCaneda ChristineRuderisch NadineDeng ShuyunLiddelow Shane A,

Zhang ChaolinDaneman RichardManiatis TomBarres Ben A, Wu Jia Qian. An RNA-Sequencing Transcriptome and Splicing Database of Glia, Neurons, and Vascular Cells of the Cerebral Cortex. The Journal of Neuroscience. 2014; 34:11929–47. [PubMed: 25186741]

Zhu X, Levasseur PR, Michaelis KA, Burfeind KG, Marks DL. A distinct brain pathway links viral RNA exposure to sickness behavior. Sci Rep. 2016; 6:29885. [PubMed: 27435819]

Highlights

- TRIFKO mice have attenuated sickness behavior after LPS exposure.
- TRIF mediates neutrophil recruitment and microglia activation after LPS exposure.
- TRIFKO mice have attenuated anorexia, muscle catabolism, and fatigue during cancer.

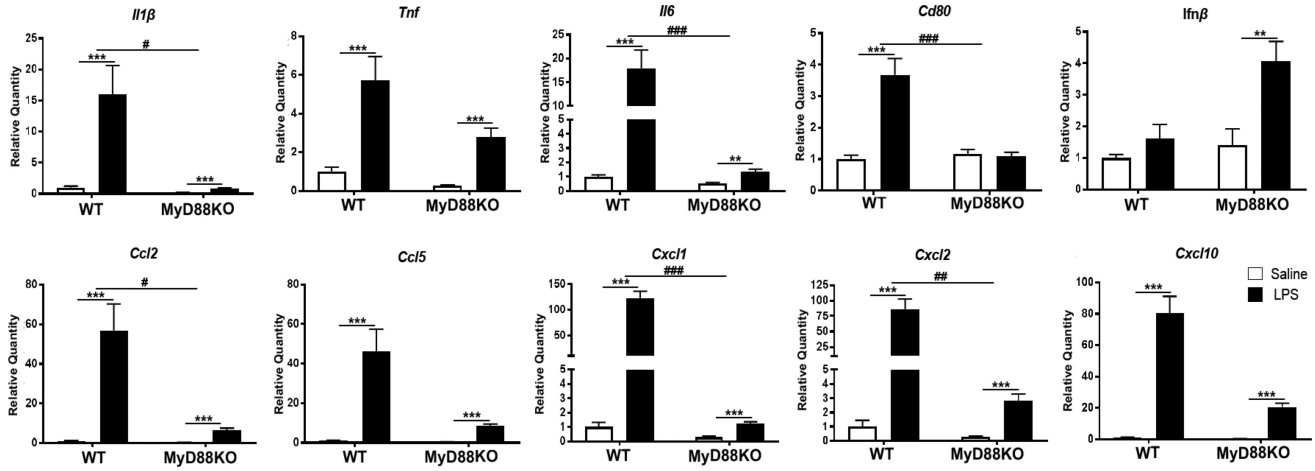

Figure 1. Mice lacking MyD88 experience hypothalamic inflammation after systemic LPS challenge

Expression of inflammatory cytokine genes in the hypothalamus 6 hrs after 250 μg/kg IP LPS treatment. ** = p<0.01, *** = p<0.001 for Two-way ANOVA Bonferroni post hoc comparisons comparing saline-treated animals to LPS-treated animals within the same genotype. # = p<0.05, ## = p<0.01, ### = p<0.001 for interaction effect in Two-way ANOVA. N = 3–5/group.

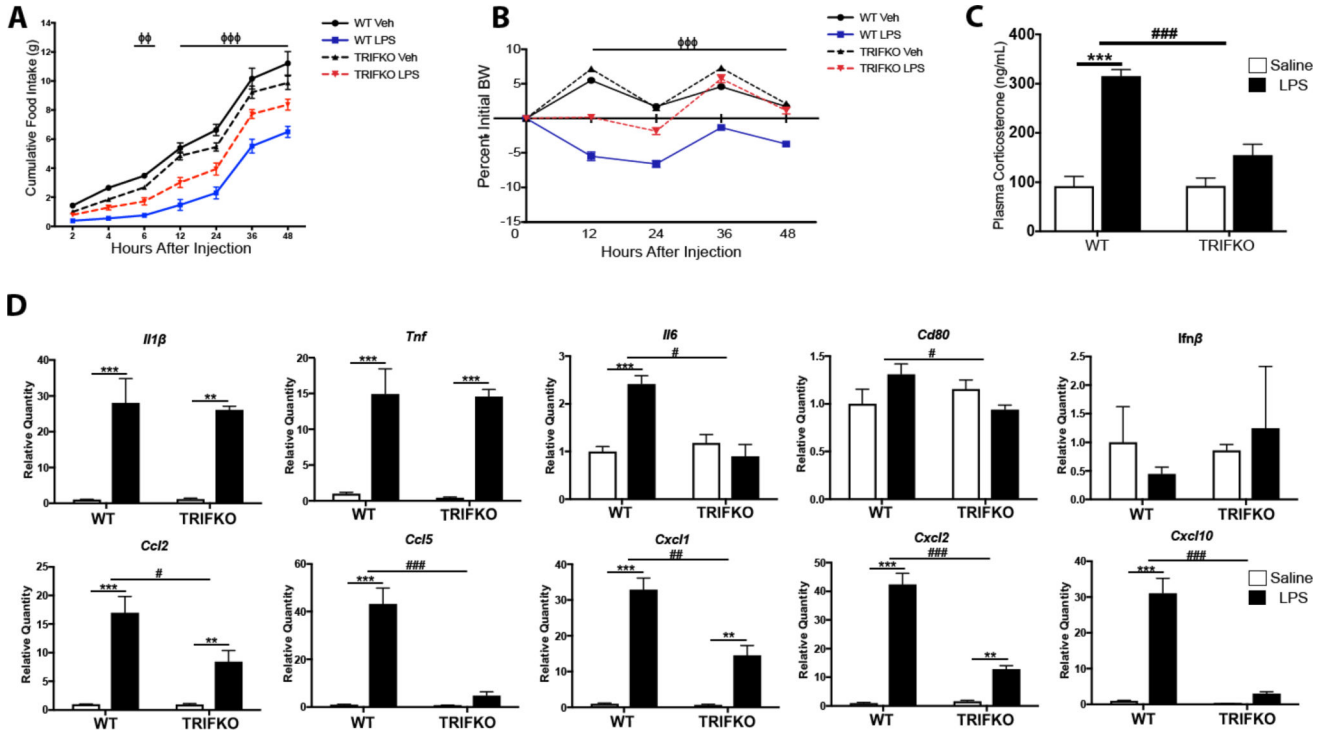

Figure 2. TRIFKO mice have attenuated acute sickness behavior in response to systemic LPS exposure

A) Cumulative food intake after 250 μg/kg IP LPS treatment. Veh = vehicle treatment (BSA/saline). ΦΦ = p<0.01 for WT LPS vs. TRIFKO LPS in Bonferroni post hoc comparisons at 6 hrs after injection, ΦΦΦ = p<0.001 for WT LPS vs. TRIFKO LPS in Bonferroni post hoc comparisons at 12, 24, 36, and 48 hrs after injection. B) Body weight change after 250 μg/kg IP LPS treatment. BW = body weight. ΦΦΦ = p<0.001 for WT LPS vs. TRIFKO LPS in Bonferroni post hoc comparisons at 12, 24, 36, and 48 hrs after injection. N = 5–7/group. C) Plasma corticosterone measurement 4 hrs after 250 μg/kg IP LPS treatment. N = 5/group. *** = p<0.001 for Bonferroni post hoc comparisons comparing saline-treated animals to LPS-treated animals within the same genotype, ### = p<0.001 for interaction effect in Two-way ANOVA. D) Expression of inflammatory cytokine genes in the hypothalamus 6 hrs after 250 μg/kg IP LPS treatment. All data are analyzed from ΔCt values and normalized to WT saline group. ** = p<0.01, *** = p<0.001 for Bonferroni post hoc comparisons comparing saline-treated animals to LPS-treated animals within the same genotype. # = p<0.05, ## = p<0.01, ### = p<0.001 for interaction effect in Two-way ANOVA. N = 3–4/group. One outlier was removed in the TRIFKO LPS groups due to complete lack of behavioral response to LPS.

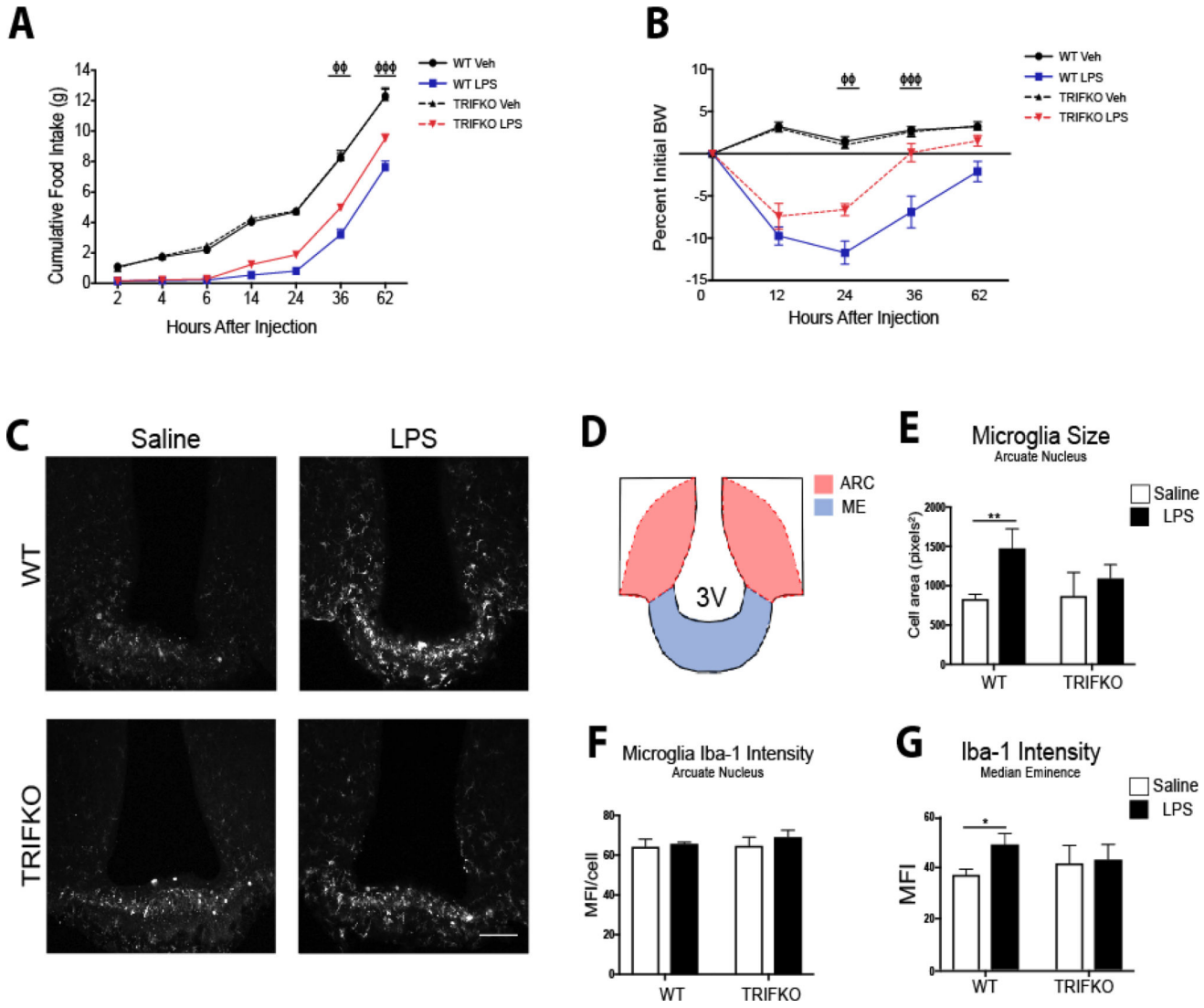

Figure 3. TRIFKO mice have attenuated acute sickness behavior in response to central nervous system LPS exposure

A) Cumulative food intake after 50 ng ICV LPS treatment. Veh = vehicle treatment. B) Body weight change after 50 ng ICV LPS treatment. BW = body weight. For A and B ΦΦ = $p<0.05$, ΦΦΦ = $p<0.001$ for WT LPS vs. TRIFKO LPS in Two-Way ANOVA Bonferroni post hoc comparisons. N = 5–6/group. C) Representative images of Iba-1 immunoreactivity in 200× magnification images of the MBH in WT and TRIFKO mice after either 50 ng ICV LPS or saline. Scale bar = 100 μm. D) Cartoon of MBH depicting regions of interest for quantification. ARC = arcuate nucleus, ME = median eminence. E) Quantification of arcuate nucleus microglia size (area) in pixels^2 after either ICV LPS or saline. F) Quantification of Iba-1 intensity per microglia in the arcuate nucleus in WT and TRIFKO mice after either ICV LPS or LPS saline. G) Quantification of Iba-1 intensity in the median eminence in WT and TRIFKO mice after either ICV LPS or LPS saline. For E–G * = $p<0.05$, ** = $p<0.01$ for Bonferroni post hoc comparisons comparing saline-treated animals to LPS-treated animals within the same genotype. n = 4/group.

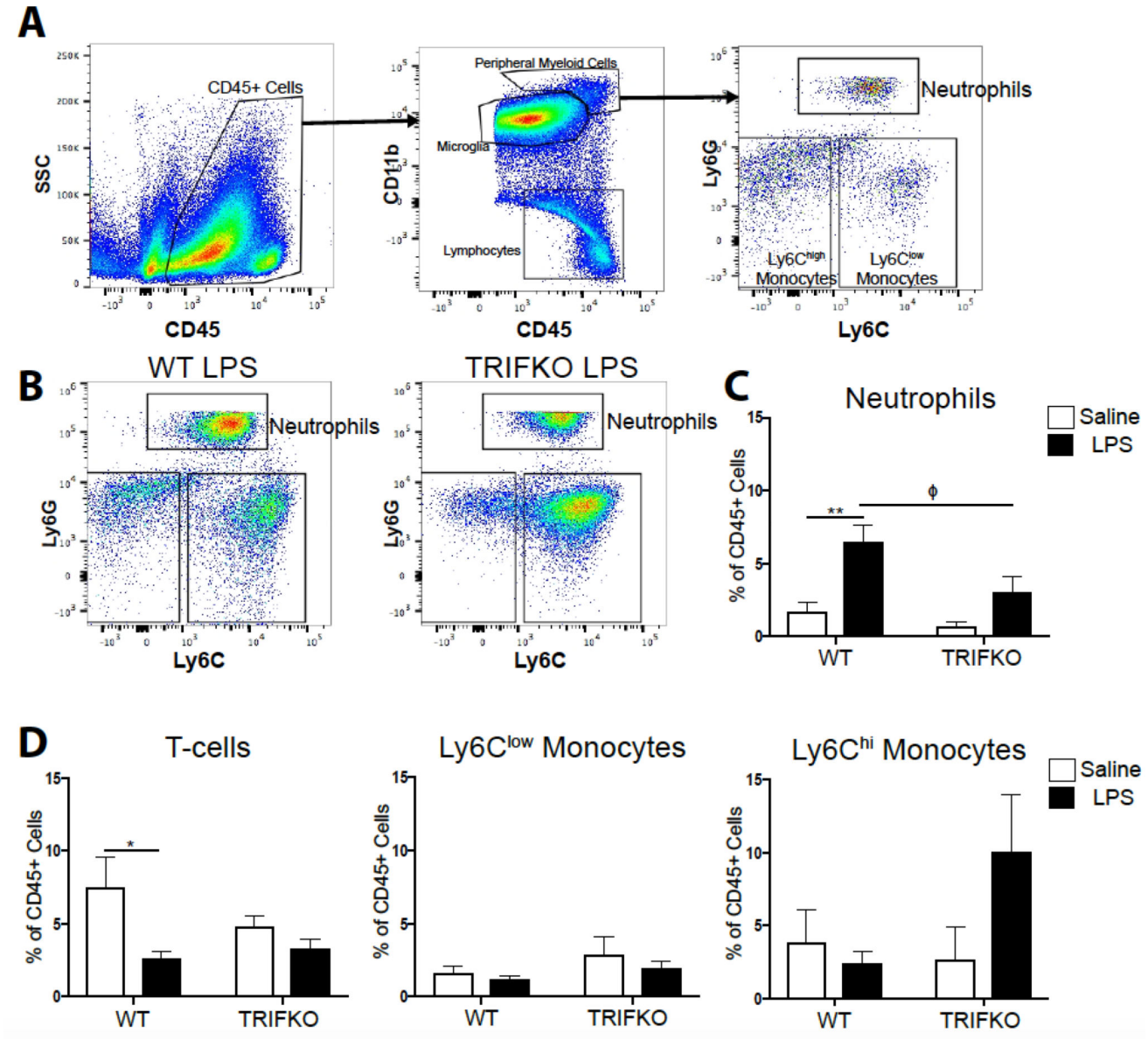

Figure 4. TRIF is required for neutrophil recruitment to the brain after ICV LPS

A) Flow cytometry gating strategy for various immune cell types in the brain from representative WT brain treated with ICV saline. B) Representative flow cytometry plots from WT and TRIFKO brains treated with 500 ng ICV LPS, gated for $CD45^{high}$ CD11b+ myeloid cells. Note that the population defined as neutrophils ($Ly6C^{mid}Ly6G^{high}$) may appear compressed in the TRIFKO LPS plot. This is due to the wide range of Ly6G expression on neutrophils, and a nonsignificant increase in Ly6G expression in brain-infiltrating neutrophils in LPS-treated TRIFKO mice (Figure S3). As a result, some neutrophils reached the pre-defined "maximum" fluorescent intensity ($10^{5.5}$). Any cells with a Ly6G fluorescent intensity greater than this were assigned a fluorescent intensity of $10^{5.5}$. As shown in Figure S3, all such events were still counted as "neutrophils" in quantitative analysis. C) Quantification of neutrophils in the brain as percentage of total CD45+ in WT and TRIFKO brains treated with either ICV LPS or saline. ** = $p<0.01$ for comparing

saline-treated to LPS-treated animals within the same genotype, Φ = p <0.05 for WT LPS vs. TRIFKO LPS in Bonferroni post hoc comparisons. D) Quantification of CD3+ T-cells, $Ly6C^{low}$ monocytes, and $Ly6C^{hi}$ monocytes in the brain as percentage of total CD45+ in WT and TRIFKO brains treated with either ICV LPS or saline. * = p<0.05, for comparing saline-treated to LPS-treated animals within the same genotype in Bonferroni post hoc comparisons. N = 4/group.

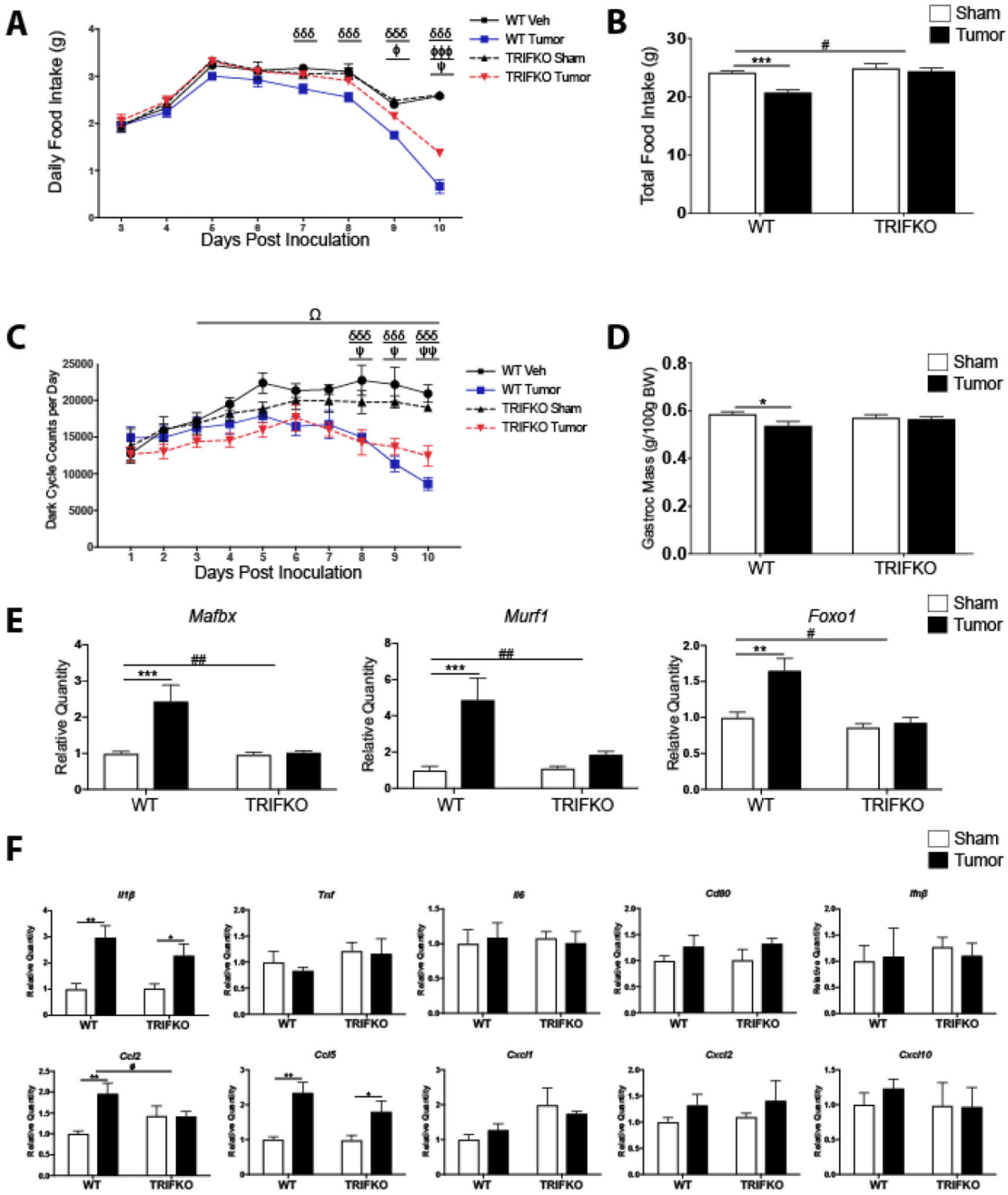

Figure 5. TRIFKO mice have attenuated cancer cachexia

A) Daily food intake after a single orthotopic inoculation of $3e^6$ KPC tumor cells. δδδ = p<0.001 for WT sham vs. WT tumor in Bonferroni post hoc comparisons. Φ = p<0.05, ΦΦΦ = p<0.001 for WT tumor vs. TRIFKO tumor in Bonferroni post hoc comparisons. Ψ = p<0.05 for TRIFKO sham vs. TRIFKO tumor in Bonferroni post hoc comparisons. B) Cumulative food intake 10 days post inoculation. *** = p<0.001 for WT sham vs. WT tumor in Bonferroni post hoc comparisons. # = p<0.05 for interaction in Two-way ANOVA. C) Movement quantification after inoculation with KPC tumor cells. Movement quantified using a Minimitter system with e-mitter implanted subcutaneously in between shoulder

blades. δδδ = p<0.001 for WT sham vs. WT tumor in Bonferroni post hoc comparisons. Ψ = p<0.05, ΨΨ = p<0.01 for TRIFKO sham vs. TRIFKO tumor in Bonferroni post hoc comparisons. Ω = p<0.05 for Three-way ANOVA interaction effect between genotype and treatment for days 3–10 post inoculation. D) Muscle catabolism determined by gastrocnemius mass. Mass of dissected left and right gastrocnemius was averaged and then divided by initial body weight for normalization. * = p<0.05 for WT sham vs. WT tumor in Bonferroni post hoc comparisons. E) qRT-PCR analysis of muscle catabolism genes in gastrocnemius. Expression level for all groups was normalized to WT sham. ** = p<0.01, *** = p<0.001 for WT sham vs. WT tumor in Bonferroni post hoc comparisons. # = p<0.05, ## = p<0.01 for interaction effect in Two-way ANOVA. F) Expression of inflammatory cytokine genes in the hypothalamus 10 days after orthotopic inoculation with KPC tumor cells. All data are analyzed from ΔCt values and normalized to WT sham group. * = p<0.05, ** = p<0.01, for WT sham vs. WT tumor in Bonferroni post hoc comparisons. # = p<0.05, for interaction effect in Two-way ANOVA. N = 5/group for all experiments. Data are representative from 3 independent experiments.